

## Aminopyrazole–Phenylalanine Based GPR142 Agonists: Discovery of Tool Compound and in Vivo Efficacy Studies

Ming Yu,<sup>\*,†</sup> Mike Lizarzaburu,<sup>†</sup> Alykhan Motani,<sup>†</sup> Zice Fu,<sup>†</sup> Xiaohui Du,<sup>†</sup> Jiwen (Jim) Liu,<sup>†</sup> Xianyun Jiao,<sup>†</sup> SuJen Lai,<sup>†</sup> Peter Fan,<sup>†</sup> Angela Fu,<sup>†</sup> Qingxiang Liu,<sup>†</sup> Michiko Murakoshi,<sup>‡</sup> Futoshi Nara,<sup>‡</sup> Kozo Oda,<sup>‡</sup> Ryo Okuyama,<sup>‡</sup> Jeff D. Reagan,<sup>†</sup> Nobuaki Watanabe,<sup>‡</sup> Mami Yamazaki,<sup>‡</sup> Yumei Xiong,<sup>†</sup> Ying Zhang,<sup>†</sup> Run Zhuang,<sup>†</sup> Daniel C.-H. Lin,<sup>†</sup> Jonathan B. Houze,<sup>†</sup> Julio C. Medina,<sup>†</sup> and Leping Li<sup>†,§</sup>

<sup>†</sup>Amgen Inc., 1120 Veterans Boulevard, South San Francisco, California 94080, United States

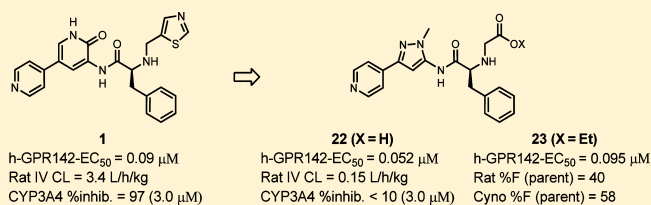
<sup>‡</sup>Daichi-Sankyo, 1-2-58 Hiromachi, Shinagawa-Ku, Tokyo 140-8710; 1-16-13 Kitakasai, Edogawa-Ku, Tokyo 134-8650, Japan

## Supporting Information

**ABSTRACT:** Herein, we report the lead optimization of amrinone–phenylalanine based GPR142 agonists. Structure–activity relationship studies led to the discovery of aminopyrazole–phenylalanine carboxylic acid **22**, which exhibited good agonistic activity, high target selectivity, desirable pharmacokinetic properties, and no cytochrome P450 or hERG liability. Compound **22**, together with its orally bioavailable ethyl ester prodrug **23**, were found to be suitable

for in vivo proof-of-concept studies. Compound **23** displayed good efficacy in a mouse oral glucose tolerance test (OGTT). Compound **22** showed GPR142 dependent stimulation of insulin secretion in isolated mouse islets and demonstrated a statistically significant glucose lowering effect in a mouse model bearing transplanted human islets.

**KEYWORDS:** GPR142 agonist, type 2 diabetes, aminopyrazole–phenylalanine, insulin secretagogue, prodrug, oral glucose tolerance test, human islet transplant



GPR142, a new member in the super family of seven-transmembrane G-protein-coupled receptors (GPCRs), was first reported in 2003 by Schioth and colleagues,<sup>1</sup> and further characterized by Schaller in 2006.<sup>2</sup> GPR142 is a G<sub>q</sub>-coupled receptor that was expressed predominantly in pancreatic β-cells. Activation of this receptor triggers an intracellular signal transduction pathway, which ultimately leads to β-cell insulin secretion. Tryptophan was recently identified as an endogenous ligand for GPR142.<sup>3</sup> Activation of the receptor by tryptophan was found to stimulate insulin secretion in isolated mouse islets in both a dose- and a glucose-dependent manner and was associated with improved glucose tolerance.<sup>3</sup> These findings suggested that GPR142 plays an important role in regulating insulin secretion and glucose homeostasis. This target was therefore deemed suitable for the discovery of agents for the treatment of type II diabetes with a low associated risk of hypoglycemia.

We recently reported the discovery of amrinone–phenylalanine GPR142 agonist **1** and the subsequent optimization campaign, which provided **2** for preliminary proof-of-concept studies in rodents.<sup>5</sup> While these compounds were both highly potent in a human inositol phosphate (IP) accumulation assay<sup>6</sup> (EC<sub>50</sub> = 0.090 μM for **1** and EC<sub>50</sub> = 0.058 μM for **2**), they both suffered from high in vivo clearance, with rat IV clearance of 3.4 and 5.1 L/h/kg, respectively (Figure 1). Compound **2** was also found to be a strong CYP inhibitor. While replacing the pyridone moiety of **1** with a thiadiazole ring was later

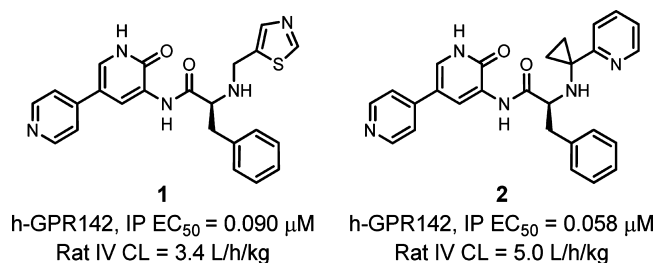


Figure 1. Structure of GPR142 agonists.

discovered to reduce rat clearance,<sup>5</sup> this heterocyclic compound was found to be chemically unstable at physiological pH conditions. Further investigation of this chemical series was therefore warranted to address the above issues and to provide a better tool compound for in vivo proof-of-concept studies.

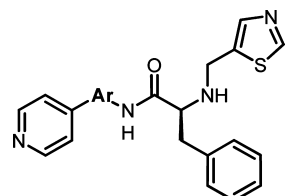
We first investigated the role of the central aromatic ring on potency as summarized in Table 1. The strategy employed was to incorporate different heterocyclic rings at the center of the molecule in order to modulate the overall shape of the molecule and optimize binding to the receptor. Isooxazole compound **3** showed a 2-fold loss in intrinsic potency (0.263

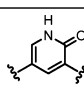
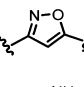
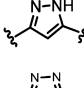
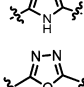
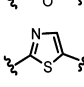
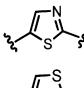
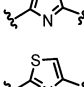
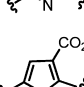
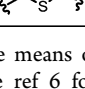
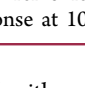
Received: March 5, 2013

Accepted: May 1, 2013

Published: May 1, 2013

Table 1. Middle Heterocyclic Ring Replacements



Compd	-Ar-	h-GPR142, IP	
		EC <sub>50</sub> , μM <sup>a,b</sup> (%Emax <sup>c</sup> )	
		Buffer	h-Serum
1		0.090 (120)	0.502 (177)
3		0.263 (107)	0.306 (114)
4		0.095 (115)	0.164 (117)
5		2.17 (90)	- <sup>d</sup>
6		>33.0 (50)	- <sup>d</sup>
7		0.090 (97)	0.161 (114)
8		0.734 (72)	1.04 (83)
9		1.081 (108)	1.11 (82)
10		0.287 (108)	0.452 (142)
11		0.121 (89)	1.25 (121)

<sup>a</sup>Values were the means of three determinations; standard deviation was  $\pm 30\%$ . <sup>b</sup>See ref 6 for assay protocol. <sup>c</sup>% Fraction of maximal tryptophan response at 10  $\mu\text{M}$ . <sup>d</sup>Not determined.

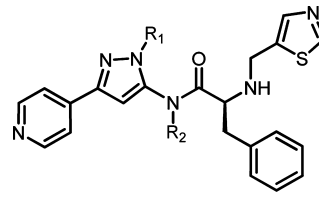
$\mu\text{M}$ ) compared with pyridone compound **1** (0.090  $\mu\text{M}$ ). This compound, however, displayed lower shift of the EC<sub>50</sub> value (0.306  $\mu\text{M}$ ) in the presence of 100% of human serum. Encouraged by this result, we explored additional analogous heterocycles. Pyrazole **4** was found to restore the EC<sub>50</sub> (0.095  $\mu\text{M}$ ) in buffer, and more interestingly, it also had low EC<sub>50</sub> shift in the presence of serum (0.164  $\mu\text{M}$ ). The 1,2,4-triazole (**5**) and 1,3,4-oxadiazole (**6**) both had significantly lower intrinsic potency. Thiazole compound **7** was as equally potent as **4** (0.090  $\mu\text{M}$ ), but the activity of similar analogues was very sensitive to the ring orientation, and none of regioisomers **8–10** showed comparable potency. Finally, thiophene compound **11** displayed a reasonable EC<sub>50</sub> in buffer (0.121  $\mu\text{M}$ ) but was 10-fold less potent in serum.

The most potent compounds (**4** and **7**) were profiled in liver microsomes (LM). Compound **4** had marginally higher percentage of compound remaining intact (8% and 33%) than **7** (3% and 5%) after incubation at 1.0  $\mu\text{M}$  for 30 min in human and rat LM, respectively. It also exhibited better LM intrinsic clearances (154 and 345  $\mu\text{L}/\text{min}/\text{mg}$  protein in human and rat, respectively) than **7** (345 and 459  $\mu\text{L}/\text{min}/\text{mg}$

protein). In in vivo pharmacokinetic studies, compound **4** displayed lower rat clearance (3.1 L/h/kg) than **7** (higher than rat liver blood flow rate). Compound **4** was therefore selected as the template for further SAR exploration.

To optimize the middle pyrazole core, various pyrazole nitrogen substitutions were investigated as illustrated in Table 2. The *N*-methyl substituent (**12**) slightly improved the

Table 2. Pyrazole Ring Modification



compd	R <sub>1</sub>	R <sub>2</sub>	h-GPR142, IP EC <sub>50</sub> (μM) <sup>a,b</sup>	rat LM <sup>c</sup> % remain
4	-H	H	0.095	33
12	-CH <sub>3</sub>	H	0.037	8
13	-CH <sub>2</sub> CF <sub>3</sub>	H	0.180	9
14	-CH <sub>2</sub> CH <sub>2</sub> -		2.78	1
15	-CH <sub>2</sub> CO <sub>2</sub> H	H	0.516	>90

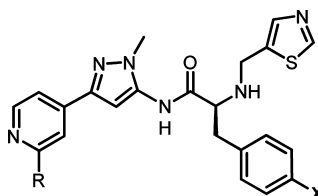
<sup>a</sup>Values were the means of three determinations; standard deviation was  $\pm 30\%$ . <sup>b</sup>Assay in buffer; see ref 6 for assay protocol. <sup>c</sup>Percentage of compound remaining intact after incubation in rat liver microsomes (RLM) at 1.0  $\mu\text{M}$  for 30 min at 22 °C.

potency (0.037  $\mu\text{M}$ ) versus the unsubstituted pyrazole (**4**), but none of the other *N*-substituents on the pyrazole ring was as potent.<sup>7</sup> Alkyl substitution of the pyrazole nitrogen was later found to be detrimental to the metabolic stability in rat LM. The percentage of compound remaining intact dropped from 33% for **4** to 8% for **12**. Similarly, low stability in rat LM was also observed with the hydrophobic trifluoroethyl analogue **13** (9%). Conformational rigidification was attempted as exemplified by **14**, but locking the 5-amino-pyrazole into coplanar conformation led to significant loss of potency (2.78  $\mu\text{M}$ ) without any stability benefit (1%). Interestingly the carboxy-containing pyrazole **15** markedly improved the stability in rat LM (>90%). Since good stability was also observed previously on another carboxylic acid compound **11** (63%) (Table 1), we hypothesized that the physicochemical nature of a carboxylic acid protects the molecule from microsomal metabolism.

Concurrent SAR campaign on the aminopyridone lead **1** revealed that  $\alpha$ -methylamino substitution of the naked pyridine ring was able to improve the metabolic stability of the compound.<sup>4,5</sup> This modification was incorporated into the aminopyrazole lead series (Table 3) and improved the stability from 8% of **12** to 38% of **16** in rat LM. The CYP inhibitory activity was also notably reduced (86% of **16** vs 16% of **12**) with this optimization. It should also be noted that *para*-fluorination of the phenylalanine ring (**17**) provided a marginal improvement of stability in rat LM (49%). These modifications were therefore integrated into the template for our next optimization.

A breakthrough in the metabolic stability of the series was made when we manipulated the physicochemical properties of the molecule through substitution of the phenylalanine nitrogen. As highlighted in Table 4, introduction of acidic amino substituents as exemplified by 1,2,3-triazole **18**, tetrazole **19**, and acetic acid **20** resulted in an increase in compound stability in rat LM. These improvements were also reflected in

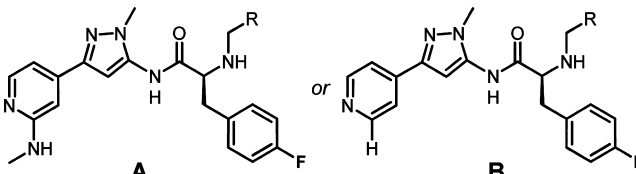
Table 3. Elimination of CYP Inhibitory Activity



compd	-R	-X	h-GPR142, IP EC <sub>50</sub> (μM) <sup>a,b</sup>	RLM % remain <sup>c</sup>	CYP3A4 % activity <sup>d</sup>
12	-H	-H	0.037	8	16
16	-NHCH <sub>3</sub>	-H	0.037	38	86
17	-NHCH <sub>3</sub>	-F	0.049	49	71

<sup>a</sup>Values were the means of three determinations; standard deviation was  $\pm 30\%$ . <sup>b</sup>See ref 6 for assay protocol. <sup>c</sup>Percentage of compound remaining intact after incubation in rat liver microsomes (RLM) at 1.0  $\mu\text{M}$  for 30 min at 22 °C. <sup>d</sup>Percentage of CYP activity remaining after incubation with compound at 3.0  $\mu\text{M}$ .

Table 4. Improvement of Metabolic Stability



Compd	R	h-GPR142, IP EC <sub>50</sub> (μM) <sup>a,b</sup>	RLM % remain <sup>c</sup>	Rat CL (L/h/kg) <sup>d</sup>
17 (A)		0.049	49	- <sup>e</sup>
18 (A)		0.026	90	6.0
19 (A)		0.071	>90	1.7
20 (A)		0.042	>90	1.0
21 (A)		0.078	<10	7.8
22 (B)		0.052	>90	0.15
23 (B)		0.095	<5%	- <sup>e</sup>

<sup>a</sup>Values were the means of three determinations; standard deviation was  $\pm 30\%$ . <sup>b</sup>See ref 6 for assay protocol. <sup>c</sup>Percentage of compound remaining intact after incubation in rat liver microsomes (RLM) at 1.0  $\mu\text{M}$  for 30 min at 22 °C. <sup>d</sup>The compounds were IV dosed at 0.5 mg/kg. <sup>e</sup>Not determined.

the gradual decrease of rat IV clearances. Equally as important was that compounds 18–20 also maintained potency on GPR142, with EC<sub>50</sub> ranging from 0.026 to 0.071  $\mu\text{M}$ . The glycine derivative 20 represented a desirable confluence of good potency (0.042  $\mu\text{M}$ ), high RLM stability (>90%), and low in vivo rat clearance (CL = 1.0 L/h/kg). Amide 21 was also prepared, but it was found to be metabolically unstable. Furthermore, with the new acetic acid feature, it was found that the amino substitution on the pyridine and the 4-fluoro of the phenylalanine as in compound 20 were no longer necessary for desirable metabolic stability. Compound 22, after removal of

these fragments, was also found to be metabolically stable and free from inhibitory activity against CYP450 isoforms 3A4 and 2D6 (IC<sub>50</sub> > 30  $\mu\text{M}$  for both).

Compound 22 was further evaluated in both in vitro and in vivo experiments. In addition to good activity on human, 22 exhibited a GPR142-EC<sub>50</sub> of 0.031 and 0.079  $\mu\text{M}$  in mouse and cynomolgus monkey, respectively, albeit in slightly lower maximum efficacy (73% and 79%, respectively). It was equally stable in human LM (>90%) as in rat. Low in vivo clearance (0.15 L/h/kg) and reasonable half-life (4.1 h) were observed in rats. In plasma, compound 22 had an unbound fraction of 16% in human, 10% in cynomolgus monkey, and 1% in rat. This compound did not show hPXR activation and was also devoid of hERG liability (IC<sub>50</sub> > 30  $\mu\text{M}$ , PatchClamp assay).

Compound 22 was tested in an ex vivo experiment for its ability to stimulate insulin secretion directly from isolated mouse islets. As illustrated in Figure 2, compound 22 stimulated insulin secretion from wild-type but not GPR142 deficient islets. These results indicated that the activity of compound 22 was specific to GPR142.

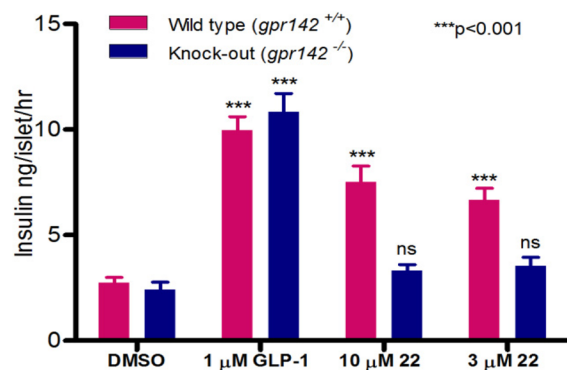


**Figure 2.** Insulin secretion stimulation test of 22 on isolated mice islets; islets isolated from wild-type and GPR142 knockout mice were incubated with 3.0 and 10.0  $\mu\text{M}$  concentrations of 22 in the presence of 16.7 mM glucose; insulin secreted into the media was quantified by ELISA (ALPCO); mean + SEM,  $n = 4$ ; statistics by  $t$  test vs wild-type; ns = not significant.

Further profiling revealed that compound 22 had low permeability across a Caco-2 monolayer ( $0.9 \times 10^{-6}$  cm/s). The poor permeability, presumably due to the zwitterionic nature of the molecule, resulted in low oral bioavailability (3% in rat at 2.0 mg/kg and 6% in cynomolgus monkey at 10.0 mg/kg). Subcutaneous (SC) administration of the compound at 2.0 mg/kg overcame this hurdle with 81% bioavailability in rat and a maximal drug concentration ( $C_{\text{max}}$ ) of 7.5  $\mu\text{M}$ . Similar level of drug exposure was also observed in cynomolgus monkey at the same SC dosage ( $F = 100\%$ ,  $C_{\text{max}} = 6.3 \mu\text{M}$ ).

In order to develop an orally bioavailable tool compound, we turned to a prodrug strategy and studied the ethyl ester analogue 23 (Table 5). After po administration of 23 at 2.0 mg/kg in rats, a 40% bioavailability of the parent acid 22 was achieved with  $C_{\text{max}}$  of 6.8  $\mu\text{M}$ . The compound exposure correlated well with escalating prodrug dosage and gave a  $C_{\text{max}}$  of 150  $\mu\text{M}$  in rats at 30.0 mg/kg. Similarly, in cynomolgus monkeys, prodrug 23 at 2.0 mg/kg delivered free acid 22 in 58% bioavailability with  $C_{\text{max}}$  reaching 2.5  $\mu\text{M}$ . Dosing cynomolgus monkeys at 10 mg/kg gave a  $C_{\text{max}}$  as high as 12.0  $\mu\text{M}$  and provided unbound drug concentration 15-fold over the cyno EC<sub>50</sub> (0.079  $\mu\text{M}$ ) in the IP assay.

Table 5. Pharmacokinetic Profile of Tool Compound 22 and Prodrug 23

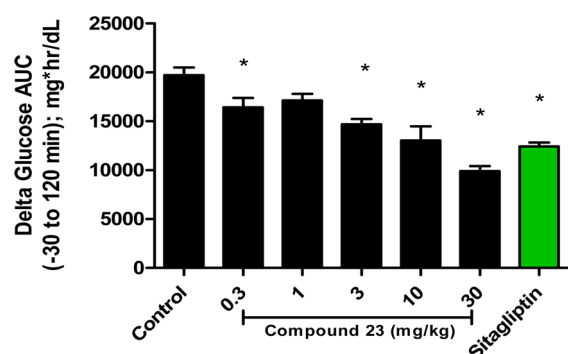
**22** (X = H)  
h-GPR142, IP EC<sub>50</sub> = 0.052 μM

**23** (X = Et)  
h-GPR142, IP EC<sub>50</sub> = 0.095 μM

species	route (compd)	dosage (mg/kg)	pharmacokinetic (PK) profile					
			Cl (L/h/kg)	t <sub>1/2</sub> (h)	V <sub>dss</sub> (L/kg)	C <sub>max</sub> (μM)	t <sub>max</sub> (h)	F (%)
rat	i.v. (22)	0.5	0.15	4.1	0.29			
	p.o. (22)	2.0				0.17	0.83	3
	s.c. (22)	2.0				7.5	0.38	81
	p.o. (23) <sup>a</sup>	2.0				6.8	0.67	40
	p.o. (23) <sup>a</sup>	30.0				150	0.50	80
mouse	p.o. (23) <sup>a</sup>	10.0				6.7	0.41	
cyno	i.v. (22)	0.5	0.44	2.3	0.33			
	p.o. (22)	10.0				0.40	4.0	6
	s.c. (22)	2.0				6.3	0.50	100
	p.o. (23) <sup>a</sup>	2.0				2.5	1.50	58
	p.o. (23) <sup>a</sup>	10.0				12.0	0.83	35

<sup>a</sup>Prodrug 23 was dosed; analytical calculations were based on parent-free acid 22.

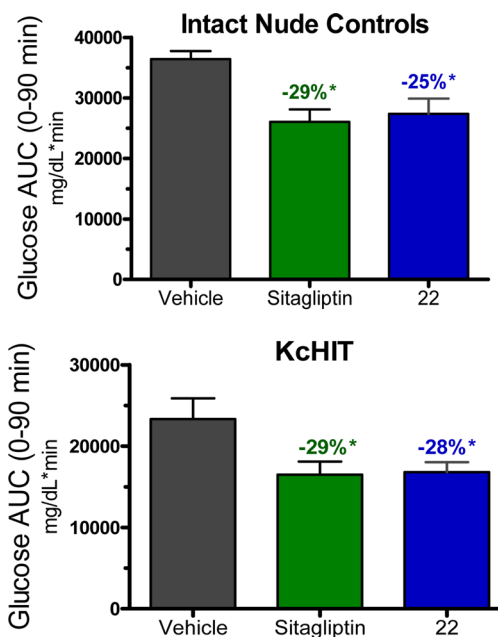
Compounds 22 and 23 were both evaluated in mice for in vivo proof-of-concept studies. The first experiment was conducted with prodrug 23 in B6 mice that were fasted overnight.<sup>8</sup> Sitagliptin (DDP-IV inhibitor) was chosen as the positive control at an oral dose of 10.0 mg/kg.<sup>9,10</sup> Total change in plasma glucose AUC (−30 to 120 min relative to glucose challenge) as shown in Figure 3 indicated a strong, dose-



**Figure 3.** Oral glucose tolerance test of 23 in mice;  $n = 8$  for control group, and  $n = 4$  for each dose group; plasma glucose excursion was monitored by blood sample collection and analysis (AccuChek glucometer) at −30, 0, 20, 40, 60, 90, and 120 min after the glucose challenge; delta AUC calculated with plasma glucose baseline level at a time point of 30 min before glucose challenge; mean + SEM; \* $p < 0.05$  vs control by 1-way ANOVA.

dependent glucose lowering effect. Direct comparison of the positive control and the 10.0 mg/kg group suggested equivalent efficiency of 23 and sitagliptin in lowering blood glucose level.

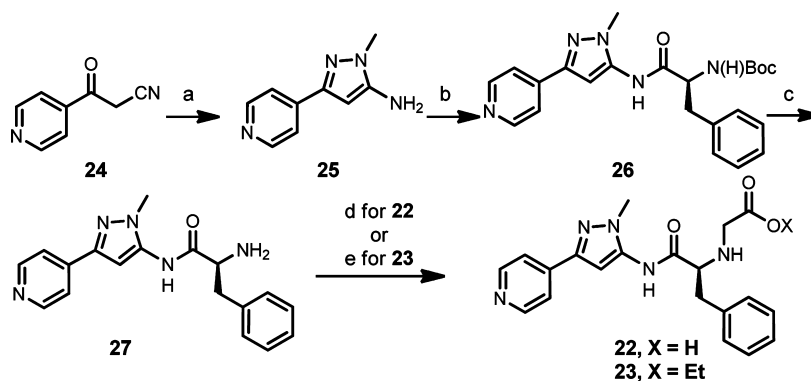
Compound 22 was also used as a tool compound (SC) for oral glucose tolerance tests<sup>11</sup> that were conducted in an intact nude mouse and a mouse model bearing human islets, transplanted under the kidney capsule (KcHIT mice).<sup>12,13</sup> As illustrated in Figure 4, direct comparison of plasma glucose AUC in the time window of 0–90 min revealed a statistically



**Figure 4.** Oral glucose tolerance test of 22 in intact vs human islet transplanted nude mice; crossover study design ( $n = 12$  for KcHIT mice and  $n = 8$  for intact nude mice, both groups were fasted for 4.0 h); mean + SEM, \* $p < 0.05$  vs vehicle by 1-way ANOVA.

significant glucose lowering effect in response to 22 in both the intact and KcHIT mice, which was similar in magnitude to a near maximal dose of sitagliptin. These data demonstrated that the efficacy of 22 was indistinguishable between human islet transplanted mice and mice that bear normal intact mouse islets. This effect was islet dependent since mice treated with streptozotocin, but without the reconstitution of healthy islets, did not exhibit glucose lowering or insulin secretion (data not shown).



Scheme 1. Synthesis of Aminopyrazole GPR142 Agonist **22** and **23**<sup>a</sup>

<sup>a</sup>Reagents and conditions: (a)  $\text{CH}_3\text{NHNH}_2$ , MeOH, conc. HCl, 60 °C, 71%; (b) Boc-L-phenylalanine, EDCI, py, DMF; (c) 20% TFA/ $\text{CH}_2\text{Cl}_2$ , 68% (two steps); (d) glyoxylic acid,  $\text{NaB}(\text{OAc})_3\text{H}$ , HOAc, 1,2-dichloroethane/dioxane, 70 °C, 42% for **22**; (e) ethyl bromoacetate, *N,N*-diisopropylethylamine, 77% for **23**.

The synthesis of the aminopyrazole–phenylalanine GPR142 agonists is exemplified by **22** as shown in Scheme 1. Treating commercially available 3-oxo-3-(pyridin-4-yl)propanenitrile **24** with methylhydrazine in the presence of concentrated HCl provided aminopyrazole **25** as the major regioisomeric product.<sup>14</sup> Amide coupling of **25** with boc-L-phenylalanine following precedent procedures<sup>4,5</sup> offered intermediate **26**. Removal of the *N*-Boc group from **26** provided the amino intermediate **27**, which after reductive amination with glyoxylic acid provided the final compound **22** in total yield of 20% after four steps. Reaction of **27** with ethyl bromoacetate under hünig base mediated condition offered the prodrug **23** in 77% yield. Similar synthetic sequences were used to provide the remainder of the compounds in this letter.

In summary, the lead optimization campaign on our aminopyrazole–phenylalanine GPR142 agonist lead series has led to the discovery of a pyrazole ring as the optimal center ring replacement, which provided compounds with good potency and low serum  $\text{EC}_{50}$  shift. The acetic acid substituent on the phenylalanine nitrogen significantly improved in vitro and in vivo metabolic stability. Tool compound **22** derived from these optimizations, together with its ethyl ester prodrug **23**, demonstrated robust in vivo efficacy through their ability to increase insulin secretion and lowering plasma glucose level. These effects were not unique to mouse native islets, but were also demonstrable in an in vivo model of human islet function. Further studies on higher species are currently in process, and the results will be published elsewhere when they become available.

## ■ ASSOCIATED CONTENT

### Ⓢ Supporting Information

Synthetic procedures and characterization data for all compounds. This material is available free of charge via the Internet at <http://pubs.acs.org>.

## ■ AUTHOR INFORMATION

### Corresponding Author

\*(M.Y.) Tel: 650-244-2050. Fax 650-837-9630. E-mail: yum@amgen.com.

### Present Address

<sup>§</sup>Presidio Pharmaceuticals, Inc., 1700 Owens Street, Suite 585, San Francisco, California 94158, United States.

## Notes

The authors declare no competing financial interest.

## ■ ACKNOWLEDGMENTS

We thank Dr. Paul Schnier for the high resonance mass spectroscopy analysis of the compounds discussed in this letter.

## ■ REFERENCES

- (1) Fredriksson, R.; Hoglund, P. J.; Gloriam, D. I.; Lagerstrom, M. C.; Schioth, H. B. Seven evolutionarily conserved human rhodopsin G protein-coupled receptors lacking close relatives. *FEBS Lett.* **2003**, *554*, 381–388.
- (2) Suesens, U.; Hermans-Borgmeyer, I.; Urny, J.; Schaller, H. C. Characterisation and differential expression of two very closely related G-protein-coupled receptors, GPR139 and GPR142, in mouse tissue and during mouse development. *Neuropharmacology* **2006**, *50*, 512–520.
- (3) Xiong, Y.; Motani, A.; Reagan, J.; Gao, X.; Yang, H.; Ma, J.; Schwandner, R.; Zhang, Y.; Liu, Q.; Miao, L.; Luo, J.; Tian, H.; Chen, J.-L.; Murakoshi, M.; Nara, F.; Yeh, W.-C.; Cao, Z. Submitted for publication.
- (4) Lizarzaburu, M.; Turcotte, S.; Du, X.; Duquette, J.; Fu, A.; Houze, J.; Li, L.; Liu, J.; Oda, K.; Okuyama, R.; Reagan, J. D.; Yu, M.; Medina, J. C. Discovery and optimization of a novel series of GPR142 agonists for the treatment of type 2 diabetes mellitus. *Bioorg. Med. Chem. Lett.* **2012**, *22*, 5942–5947.
- (5) Du, X.; Kim, Y.-J.; Lai, S.; Chen, X.; Lizarzaburu, M.; Turcotte, S.; Oda, K.; Okuyama, R.; Nara, F.; Murakoshi, M.; Fu, A.; Reagan, J.; Liu, Q.; Zhang, Y.; Motani, A.; Fan, P.; Xiong, Y.; Shen, W.; Li, L.; Houze, J.; Medina, J. C. Phenylalanine derivatives as GPR142 agonists for the treatment of Type II diabetes. *Bioorg. Med. Chem. Lett.* **2012**, *22*, 6218–6223.
- (6) Inositol Phosphate Accumulation Assay-HEK293 cells were dispensed into a poly-D-lysine tissue culture treated 96-well plate at a density of 25 000 cells per well. The next day, the cells (~80–90% confluent) were transfected with 100 ng of receptor plasmid per well using Lipofectamine2000 according to the manufacturer's instructions. Six hours after transfection the media was replaced with inositol free DMEM/10% dialyzed FCS supplemented with 1.0  $\mu\text{Ci}/\text{mL}$  tritiated inositol. After incubation overnight, the cells were washed once in HBSS and then treated with the 100  $\mu\text{L}$  HBSS/0.01% BSA containing various concentrations of test compounds (prepared as above in DMSO) and 10 mM LiCl, and incubated at 37 °C for 1 h. The media was aspirated, and the cells were lysed with ice cold 20 mM formic acid. After incubation at 4 °C for 5 h, the lysate were added to yttrium silicate SPA beads, allowed to settle overnight, and read on a Beckman

TopCount scintillation counter. In measuring the  $EC_{50}$  with serum, HBSS/0.01% BSA was replaced with 100% human serum.

(7) The investigation of pyrazole N-substitution included alkyl groups in different sizes and physicochemical properties (e.g., -Et, -<sup>n</sup>Pr, -<sup>3</sup>Pr, and -CH<sub>2</sub>CH<sub>2</sub>OH), but none of these compounds was as potent as **12**. Moving the substitution onto the other nitrogen of the pyrazole ring led to significant loss of potency.

(8) In this experiment, the animals were challenged in a single oral dose of glucose (4.0 kg/kg) at the time point of zero ( $t = 0$  min).

(9) Sitagliptin was dosed 30 min ( $t = -30$  min) before oral glucose challenge.

(10) In the pharmacokinetic study of **23** on fasted B6 mice at 10.0 mg/kg PO dosage, the plasma drug level of parent **22** was observed to reach a peak level of 6.7  $\mu$ M 25 min after dosing. Compound **23** was administrated at escalating doses of 0.3, 1.0, 3.0, 10.0, and 30.0 mg/kg, respectively, 30 min before an oral glucose challenge. The selection of this dosing timing ( $t = -30$  min) was to synchronize the drug  $t_{max}$  of each group close to the time point of glucose challenge.

(11) In this experiment, the animals were challenged in a single oral dose of glucose (4.0 kg/kg) at the time point of zero ( $t = 0$  min). Both the vehicle and the positive control sitagliptin (10.0 mg/kg) were orally administrated at -60 min. The subject compound **22** (10 mg/kg) was dosed (SC) at -15 min. The selection of dosing route and timing were to synchronize the drug  $t_{max}$  of each group close to the time point of glucose challenge. Blood glucose levels were determined (AccuChek glucometer) at time points of 0, 5, 15, 25, 30, 45, 60, and 90 min.

(12) These immunodeficient mice (to avoid rejection of the transplanted human islets) were previously treated with streptozotocin (an islet specific toxin) to eradicate endogenous mouse islets. Thus, this model allows for the evaluation of compound efficacy in an in vivo setting using human islets.

(13) Jansson, J.; Eizirik, D. L.; Pipeleers, D. G.; Hakan Borg, L. A.; Hellerstrom, C.; Andersson, A. Impairment of glucose-induced insulin secretion in human pancreatic islets transplanted to diabetic nude mice. *J. Clin. Invest.* **1996**, *96*, 721–726.

(14) For the chemical construction of compounds bearing other heterocyclic B rings as discussed in Table 1, see Supporting Information.